High-Resolution Spectroscopic Imaging Using a Deformable Spatio-Spectral Model

M. Jacob[1], T. Deller[1], N. Schuff[2], X. Zhu[2], Z-P. Liang[1]

[1]Beckman Institute, University of Illinois at Urbana-Champaign, Urbana, IL, United States, [2]DVA Medical Center and University of California, San Francisco, San Francisco, CA, United States

INTRODUCTION

Spectroscopic imaging suffers from long acquisition time due to the large number of data samples to be acquired (spatial and spectral). Most of the current approaches to Chemical Shift Imaging (CSI) sacrifice spatial resolution to perform the scan in a reasonable time. To circumvent this problem, methods such as SLIM [1], GSLIM [2], and SLOOP [3] use *a priori* information from high-resolution anatomical scans to extrapolate the spatial frequencies. However, the applicability of these methods to spectroscopic brain imaging has been limited due to various non-idealities including magnetic inhomogeneities, compartments not matching the corresponding regions in the spectroscopic scan, poor segmentation, etc.

We propose a novel method based on deformable spatio-spectral compartmental modeling. Since the new model accounts for the non-idealities, it gives a better fit to the data, avoiding basic problems such as spectral leakage inherent to many existing methods.

METHOD

A. Spatio-spectral Model: Based on the assumption that spectroscopic information is smooth in each compartment, we model each region as a linear combination of lower order exponentials (the support of the exponentials is limited to the corresponding region) for a given frequency. The resulting 3-D function is piecewise smooth:

$$\rho(\mathbf{x}, f) = \sum_{i=0}^{N-1} \sum_{l=0}^{n_i-1} c_{i,l}(f)\, \phi_{i,l}(\mathbf{x}), \qquad \mathbf{x} \in \Re^3, f \in \Re \tag{1}$$

We assume N compartments; $\phi_{i,l}(\mathbf{x})$ are the exponential-functions that are support-limited to the i-th compartment. We obtain the compartments by the segmentation of high-resolution anatomical volume data.

Due to patient motion, difference in scan protocols, and poor segmentation, misregistration between the anatomical segmentation and the spectroscopic scan may occur. Even a small mismatch can lead to severe spectral leakage from lipid regions (due to the high signal magnitude). We model the spatial mismatch as an affine transformation. Thus the deformable model is given by

$$\rho_1(\mathbf{x}, f) = \rho(\mathbf{A}\mathbf{x} + \mathbf{b}, f) \tag{2}$$

where $\mathbf{A}$ and $\mathbf{b}$ denote the affine transformation.

B. Image Formation: In the ideal set up, the FID signal is modeled as a 4-D Fourier transform of (2). However, the inhomogeneity of the magnetic field due to susceptibility differences and non-uniformity of the B_0 field results in a spatially varying shift along the frequency direction. Denoting the variation due to the inhomogeneity by $\mu(\mathbf{x}) = \gamma\Delta B(\mathbf{x})$, the forward model is the 4-D Fourier transform of

$$\rho_2(\mathbf{x}, f) = \rho(\mathbf{A}\mathbf{x} + \mathbf{b}, f - \mu(\mathbf{x})). \tag{3}$$

An estimate of the inhomogeneity is obtained either by using pilot scans or by aligning the spectral peaks to their correct locations. (The peak locations are known *a priori*. [3])

C. Algorithm: We use a steepest-descent algorithm to derive the unknown model parameters to obtain a good data-fit. Since $\mu(\mathbf{x})$ is a smooth function, we model it as a lower-order Fourier series, thereby restricting the degrees of freedom. We start the algorithm with the estimate of $\mu(\mathbf{x})$ and $\mathbf{A} = \mathbf{I}$; $\mathbf{b} = \mathbf{0}$ as initial conditions. We iteratively refine the unknowns so that the mean square error is minimized. The unknown parameters are (a) the coefficients of the affine transformation, (b) the Fourier series coefficients of $\mu(\mathbf{x})$ and (c) the coefficients $c_{i,l}(f)$. We use linear interpolation to obtain the warped function ρ_2 from ρ.

RESULTS

Our experimental CSI data (34x34x256) corresponds to a 15mm-thick slice of the brain. (There are no Fourier encodes in the z direction.) We acquired 5 high-resolution anatomical slices (thickness of 3 mm each) of the same region, and these slices are segmented individually to obtain 4 compartments (lipid, gray matter, white matter, and CSF). We also estimate the inhomogeneity map from the CSI data by aligning the spectra.

To test the algorithm, we perform 2 reconstructions: (a) assuming 16x16x256 subset of the original k-space data and (b) the full data set (34x34x256). The processing procedure is summarized below:

1. Solve for the $c_{i,l}(f)$ values from the measured data in a least-squares formulation. Generate a 64 x 64 x 5 x 256 image volume using (1).
2. Perform the spatial and frequency transformation (3) using the current parameters.
3. Compute the 3-D FFT along the spatial dimensions (since there are no Fourier encodes along the z dimension for our data, we use the sum of the 2-D FFTs of the 5 anatomical slices).
4. Calculate the error between the original measurements and the updated model.
5. Return to Step 1 and iterate until convergence.

The results are shown in Figure 1.

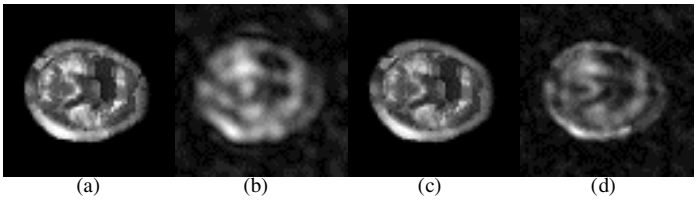

(a) (b) (c) (d)

Figure 1. Model-based versus Fourier reconstruction of the NAA peak. (a) Model based reconstruction from 16x16 k-space samples (b) Fourier reconstruction from 16x16 samples. (c) Model based reconstruction from 34x34 samples. (d) Fourier reconstruction from 34x34 samples. Note that the model based reconstructions in (a) and (c) are nearly identical, indicating that the model works well even when data is limited.

CONCLUSION

Spatial resolution of CSI can be substantially improved by incorporating anatomical MRI in a deformable spatio-spectral compartmental model as prior information. Robustness of CSI reconstruction is further improved by accounting for non-idealities, such as MRI-CSI misregistration and B_0 nonuniformity.

REFERENCES

[1] X. Hu et al., MRM, vol. 8, pp. 314-322, 1988.
[2] Z.-P. Liang et. al., IEEE TMI, pp. 132-137, 1991.
[3] R. Mejia et. al., J. Mag. Res, vol. 94, pp. 268-287, 1991.